Journal of Thermal Analysis and Calorimetry, Vol. 96 (2009) 1, 27–33

OPTIMAL SYNTHESIS OF HEAT EXCHANGER NETWORK FOR THERMOCHEMICAL S–I CYCLE

H. Liu, I. Kantor, A. Elkamel[*] *and M. Fowler*

Department of Chemical Engineering, University of Waterloo, 200 University Ave. West, Waterloo, ON, N2L3G1, Canada

In this paper, a brief survey of hydrogen production methods is presented with a focus on S–I cycle. Based on heat duty data of sulfuric acid decomposition in S–I cycle, optimization models are developed to explore the minimum utility consumption and the minimum number of heat exchangers. Finally an optimal heat exchanger network for S–I thermochemical cycle is defined by a mixed integer optimization model.

Keywords: *hydrogen, mixed integer optimization model, S–I cycle, sulfuric acid decomposition*

Introduction

Current data shows that industrial plants are becoming increasingly dependent on fossil fuels and specifically, oil. According to Statistics Canada, energy demand in Canada has increased from 7384.7 petajoules in 2002 to 7643.2 petajoules in 2006. Energy demand from transportation sector occupies about thirty percent of the total demand [1]. Automobile fuel combustion emits a large amount of air pollutants. A report published by the World Bank [2] showed that 60% of carbon monoxide emissions, and 60% of hydrocarbon emissions were from the use of passenger vehicles. The report, ‘Inventory of U.S. Greenhouse Gas Emissions and Sinks’ [3], revealed that carbon dioxide emission from the transportation sector accounted for 28% of the total carbon dioxide emission in the United States in 2006. These problems can be alleviated, at least partially, with the induction of hydrogen fuel cells onboard vehicles; creating zero-emission hydrogen fuel cell vehicles (FCVs).

Hydrogen is the lightest and the most abundant element on the earth, but pure hydrogen gas is quite rare in the natural world. Hydrogen is widely used in chemical industry. Most hydrogen is industrially produced from natural gas and coal, with the remainder being produced from the electrolysis of water. Hydrogen is considered as a green energy carrier and can be applied in hydrogen fuel cell vehicles. Some hydrogen fuel cell vehicle models have been demonstrated by the main automakers such as Phoenix model of GM, FCHV-5 model of Toyota, and FCXV-4 model of Honda [4].

Hydrogen production

Hydrogen production from natural gas

Steam-Methane Reforming (SMR) is the most common method in large scale hydrogen production, and with the current moderate natural gas price, SMR is also the least expensive method. Efficiency of this process is typically between 65 and 80% [5]. SMR processing consists of a series of chemical reactions [6], of which the two most important reactions are shown below:
steam-methane reforming reaction:

$$CH_4+H_2O \rightarrow CO+3H_2 \quad (1)$$

water-gas shift reaction:

$$CO+H_2O \rightarrow CO_2+H_2 \quad (2)$$

Hydrogen is stripped from methane and water molecules while the residual elements combine to form carbon dioxide. Carbon dioxide is produced as a by-product. Steam-methane reforming is, therefore, an unattractive method to produce ‘clean’ energy storage medium, free from CO_2 emissions. Due to these facts, hydrogen production from electrolysis using energy from renewable or nuclear sources is observed as a preferential option for hydrogen production in the future.

Water electrolysis

Hydrogen is generated by an electric current whereby water is split into hydrogen and oxygen. Water electrolysis is a very common way to generate high purity hydrogen for lab usages, but the main disad-

---

[*] Author for correspondence: aelkamel@cape.uwaterloo.ca

1388–6150/$20.00

Akadémiai Kiadó, Budapest, Hungary
Springer, Dordrecht, The Netherlands

vantage of the method is that the overall thermal-to-hydrogen conversion efficiency is relatively low. The overall conversion efficiency is the product of the individual efficiencies of electricity generation and water electrolysis. A report of the National Renewable Energy Laboratory showed that energy efficiency of the entire water electrolysis system ranged from 56–73% [7]. According to a study from the European Environment Agency, the average energy efficiency of conventional thermal electricity generation in EU25 was 38.2% in 2004 [8]. Since this time, however, some advances have been made to improve conventional power generation efficiency. The application of combined cycle gas turbine plants could increase the conversion efficiency of electricity generation to approximately 60% [8]. By applying this technology, the overall thermal-to-hydrogen conversion efficiency using water electrolysis could be expected to achieve 30–40% in the future.

High temperature electrolysis

Steam is split into hydrogen and oxygen at high temperature, utilizing large quantities of electricity and heat. If coupled with the high temperature advanced nuclear reactor, the efficiency of HTE could be expected to achieve 45–55% [9].

Thermochemical hydrogen production methods

In thermochemical cycles, water is split into hydrogen and oxygen by high temperature; typically, and reaction temperature is over 750°C [10]. Since the 1960’s, over 100 thermochemical cycles have been studied [11], but currently researchers mainly concentrate on three cycles, namely: sulphur–iodine (S–I), Calcium–bromine–iron (UT-3) and copper–chlorine (Cu–Cl). Efficiencies of thermochemical processes could be expected to exceed 40%. Reactions of thermochemical cycles are given below:
Ca–Br–Fe (UT-3) cycle [12]

$$CaBr_2+H_2O \rightarrow CaO + 2HBr \text{ (730°C)} \quad (3)$$

$$CaO + Br_2 \rightarrow CaBr_2 + 1/2O_2 \text{ (550°C)} \quad (4)$$

$$Fe_3O_4+8HBr \rightarrow 3FeBr_2+4H_2O+Br_2 \text{ (220°C)} \quad (5)$$

$$3FeBr_2+4H_2O \rightarrow Fe_3O_4+6HBr+H_2 \text{ (650°C)} \quad (6)$$

Cu–Cl cycle [12]

$$2Cu+2HCl \rightarrow 2CuCl+H_2 \text{ (450°C)} \quad (7)$$

$$4CuCl+4Cl^- \rightarrow 4CuCl_2^- \text{ (30°C)} \quad (8)$$

$$4CuCl_2^- \rightarrow 2CuCl_2 + 2Cu+4Cl^- \text{ (30°C)} \quad (9)$$

$$2CuCl_2(aq) \rightarrow 2CuCl_2(s) \text{ (100°C)} \quad (10)$$

$$2CuCl_2+H_2O \rightarrow CuO+CuCl_2+2HCl \text{ (400°C)} \quad (11)$$

$$CuO+CuCl_2 \rightarrow 2CuCl+1/2O_2 \text{ (500°C)} \quad (12)$$

The S–I cycle consists of three sections [13]:
Bunsen reaction:

$$I_2+SO_2+2H_2O \rightarrow 2HI+H_2SO_4 \text{ (120°C)} \quad (13)$$

Decomposition of sulfuric acid:

$$H_2SO_4 \rightarrow 1/2O_2+SO_2+H_2O \text{ (850°C)} \quad (14)$$

Decomposition of hydrogen iodide:

$$2HI \rightarrow H_2+I_2 \text{ (450°C)} \quad (15)$$

Overall reaction

$$2H_2O \rightarrow 2H_2+O_2 \quad (16)$$

The Bunsen reaction is the central reaction of the cycle to produce sulfuric acid and hydrogen iodide. Oxygen is produced in reaction 14, and hydrogen is produced in reaction 15. Sulfur dioxide and iodine from decomposition of hydrogen iodide and sulfuric acid are fed back to Bunsen reaction.

The S–I cycle was first invented at General Atomics in the 1970s. It has since become a promising cycle for hydrogen production by thermochemical methods. The study at General Atomics [14] shows that the efficiency of the S–I cycle can achieve 42% at 827°C and based on the result of the study, the efficiency can be predicted to exceed 50% at 900°C. Some research agencies and labs, such as: Japan Atomic Energy Agency, French CEA, General Atomic and Sandia National Laboratories have already started studies on the S–I cycle.

Overall, compared with other methods, water electrolysis and high temperature electrolysis, due to losses associated with electricity generation, are less efficient methods of hydrogen production. Relative to other energy conversion processes, thermochemical cycles have the potential to be the most efficient method for hydrogen production; however, the expectation of high efficiency would require experimental verification.

Conceptual process of S–I cycle

As illustrated in Fig. 1, sulfuric acid and hydrogen iodide are produced by Bunsen reaction in Section I. The resulting mixture of H_2SO_4 and HI is transferred into a phase separator. With the addition of excessive iodine, sulfuric acid and hydrogen iodide are separated from each other. Sulfuric acid, at the upper part of the phase separator, is fed to Section II, while HI at the bottom of the separator is transferred to Section III.

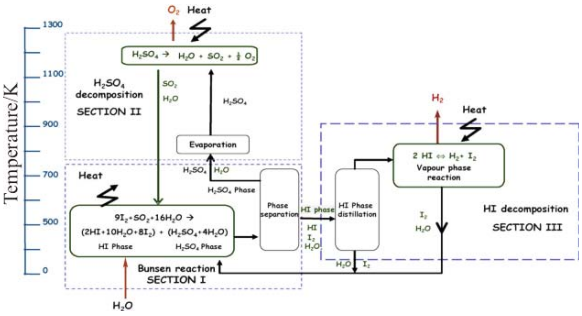

Fig. 1 Conceptual process of S–I cycle [15]

In section II, the sulfuric acid solution is concentrated by evaporation, and is then decomposed into SO_2, H_2O and O_2. SO_2 and H_2O are sent back to the Bunsen reaction, while O_2 is vented to the atmosphere or can be extracted as a by-product. In Section III, HI is separated from the mixture of HI and I_2, and then is decomposed into H_2 and I_2 in the reactive distillation column. H_2 is extracted as a product, while I_2 is reused into Section I.

Thermochemical cycles are all conducted at high temperature. Therefore the efficiency of the reactions mainly relies on the availability of heat. Through exchanger network heat integration, a large amount of heat can be saved and the efficiency of reaction can be increased. In this paper, heat integration is implemented in section II because most of the heat in the S–I cycle is consumed in this section.

Heat integration of sulfuric acid decomposition process

The report published by General Atomics [16] demonstrated the preliminary process design of hydrogen production using the S–I cycle. The heat integration will be based on the data from the decomposition process of sulfuric acid, which was developed by researchers at the University of Kentucky [16].

Description of sulfuric acid decomposition [16]

As illustrated in Fig. 2, the sulfuric acid from Section I is first concentrated in a high pressure four-stage isobaric concentrator. At each stage, the sulfuric acid is heated and water is boiled off. Following this, the acid becomes further concentrated in a set of three flash tanks and a vacuum distillation column. Thus, the sulfuric acid is highly concentrated and is ready for the decomposition process. Prior to entering the decomposition section, H_2SO_4 is preheated and evaporated at the specific temperature by a series of heat exchangers. During decomposition, H_2SO_4 is split into SO_2, O_2 and H_2O. SO_2 and H_2O are sent back to the Bunsen reaction. Some parts of O_2 will be used as a carrier gas, and the rest will be vented to the atmosphere or harnessed for purification and sale.

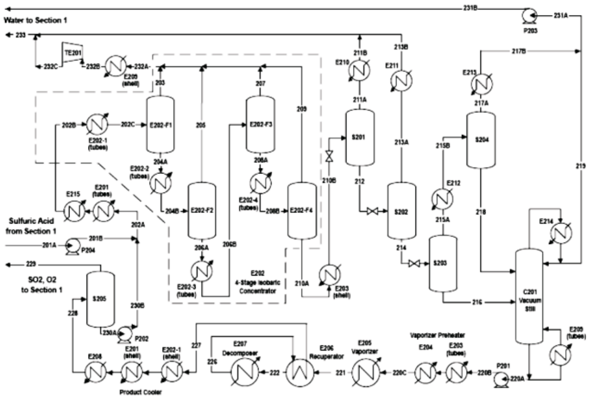

Fig. 2 The flowsheet of sulfuric acid decomposition process [16]

Principles of heat integration

The integration of heat exchangers network can be implemented as the following steps [17]:

- Heat duty data collection
- Select a minimum approach temperature
- Build a heat cascade diagram
- Set a transshipment model to minimize utility consumption
- Expand the transshipment model
- Add logical constraints to minimize the number of heat exchangers

Heat duty data collection

Before heat integration, data (such as heat content, and temperature range of each process stream) should be collected. Vacuum still C201 [Equipment references are to Figs 2 and 3] is crucial to the sulfuric

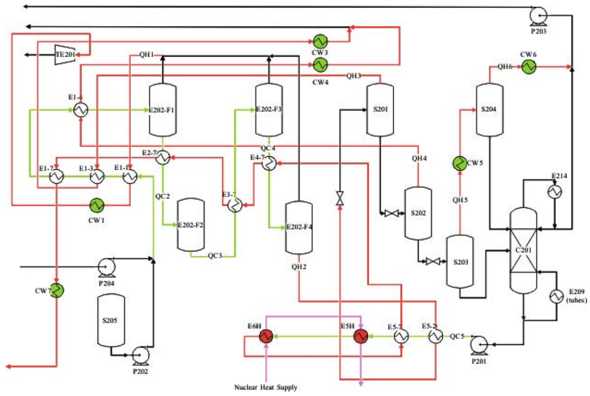

Fig. 3 Heat exchangers network of H_2SO_4 decomposition process

acid decomposition process. The bottoms product of the distillation is fed to the sulfuric acid decomposer. The composition of the vacuum distillation output has significant influence on the sulfuric acid decomposition reaction. Independent utility supplies to reboiler E209 and condenser E214 can be advantageous to maintain the appropriate composition in the vacuum distillation output. Optimal synthesis of the heat exchanger network excludes reboiler E209 and condenser E214 based on these constraints. From the data in the report [16], all of the material streams, excluding the streams of E209 and E214, are categorized as cold or hot streams. The corresponding heat duty data and temperature ranges are listed in Table 1.

The minimum approach temperature

The minimum approach temperature represents the smallest temperature difference at the sides of cold and hot streams entering and leaving exchangers. Smaller minimum temperatures can achieve higher efficiencies of heat exchange; however, it also requires larger heat transfer areas, leading to a larger capital investment. A compromise between the high heat transfer efficiency and capital investment must be reached to obtain the optimal solution to this problem. In the original design [16], the minimum approach temperature was set at 40 degrees Celsius. To make a comparison at the same level, 40 degrees is chosen as the minimum approach temperature of the optimal heat exchanger network.

Heat exchange temperature intervals

Using the collected data, a temperature interval table is built. The cold and hot streams are represented by horizontal lines while temperature intervals are shown on the top and bottom rows. According to thermodynamic laws, heat transfer only occurs with the existence of a temperature difference. 40°C is the minimum approach temperature for heat exchange; thus, at the same temperature intervals the temperatures of hot streams must be 40 degrees higher than the

Table 1 Heat duty data of hot and cold streams

Stream no.	Heat/kW	Temperature/K	ΔT/K	F_{cp}/kW °C^{-1}
Cold stream 1	193.542	120.98	209.17	0.925285653
Total heat		330.15		
Cold stream 2	46.387	330.15	16	2.8991875
Total heat		346.15		
Cold stream 3	29.009	346.15	12	2.417416667
Total heat		358.15		
Cold stream 4	27.782	358.15	13	2.137076923
Total heat		371.15		
Cold stream 5	298.898	213.05	310.8	0.961705277
Total heat		523.85		
Cold stream 6	178.459	523.85	303.3	0.588391032
Total heat		827.15		
Hot stream 1	28.928	348.35	228.2	0.126765995
Total heat		120.15		
Hot stream 2	44.117	371.15	63	0.700269841
Total heat		308.15		
Hot stream 2	14.838	289.85	169.7	0.087436653
Total heat		244.05		
Hot stream 3	19.851	244.05	123.9	0.160217918
Total heat		120.15		
Hot stream 4	6.231	159.85	24.7	0.252267206
Total heat		135.15		
Hot stream 5	25.73	135.15	97	0.265257732
Total heat		38.15		
Hot stream 6	283.938	827.15	707	0.401609618
Total heat		120.15		

temperature of cold streams. Both hot and cold streams are listed in the corresponding temperature range. Heat contents of each stream are also shown together with their representative lines. The table demonstrates the matches between the hot and cold streams with the 40°C minimum approach temperature.

Heat cascade diagram

As is the case for a typical heat cascade diagram, cold streams are shown on the left hand side, while hot streams are on the right. At each temperature interval, heat is transferred from the specific hot streams to the corresponding cold streams, and heat residual from the interval ‘cascades’ down to the next interval. Heat can only be transferred when the hot streams are in the range of the appropriate temperature intervals. A cold stream can receive heat either from the hot streams at the same interval or an upper interval.

The transshipment model of heat exchange [18]

Hot utilities and hot streams supply heat to the cold streams, whereas cold utilities cool down the hot streams. There is also residual heat cascaded down from the upper temperature intervals. The purpose of heat integration is to minimize utility consumption from chemical processes. As a first step, the objective function of the transshipment model [18] is set to explore the minimum utility consumption. The objective function is defined as shown below:

Objective function:

$$\min.\sum_{k}\sum_{m\in S^k} QS_{mk}+\sum_{k}\sum_{n\in w^k} CW_{nk} \tag{17}$$

Constraints:

$$R_{k-1}+\sum_{m\in s^k} QS_{m}+\sum_{i\in H_K} QH_{ik}=R_k+\sum_{n\in w^k} CW_{nk}+\sum_{j\in C^k} QC_{jk} \tag{18}$$

where *QS*: heat supply from hot utilities, *CW*: heat extraction from cold utilities, *QH*: heat supply from hot streams, *QC*: heat extraction from cold streams, R^k: heat residual from temperature interval *k*, $S^k=\{m\,|$ hot utilities at temperature constraints: interval $k\}$, $W^k=\{n\,|$ cold utilities at temperature interval $k\}$, $H^k=\{i\,|$ hot stream at temperature interval $k\}$, $C^k=\{j\,|$ cold streams at temperature interval $k\}$.

The overall utility consumption is set as the objective function, and the energy balances between hot utilities/streams and cold utilities/streams are set as constraints.

According to the transshipment model, the minimum utility consumption is achieved, and the ‘pinch’ point is found at interval 12. However, the interactions between each cold stream and hot stream at every temperature interval are still unclear. The number of heat exchangers in the optimal solutions is also unknown. An expanded transshipment model is required to discover the heat transfer between each hot utility/stream and cold utility/ stream.

The expanded transshipment model

An expanded transhipment model was built to demonstrate the links between cold streams and hot streams. Every hot stream is assumed to supply heat to the cold stream or cold utility. Residual heat flows down to the next interval. In a similar way, hot utility is also assumed to transfer heat to each cold stream and leave residual heat, but considering the minimum utility consumption, there is no heat transfer from hot utility to cold utility. Thus the expanded transshipment model is written as:

Objective function

$$\min.\sum_{k}\sum_{m\in S^k} QS_{mk}+\sum_{k}\sum_{n\in w^k} CW_{nk} \tag{19}$$

Constraints

$$RH_{i,k-1}+QH_{i,k}=\sum_{j\in C^k} Q_{i,j,k}+\sum_{n\in w^k} Q_{i,n,k}+RH_{i,k} \tag{20}$$

$$RS_{m,k-1}+QS_{m,k}=\sum_{j\in C^k} QS_{m,j,k}+RS_{m,k} \tag{21}$$

$$\sum_{j\in C^k} Q_{i,j,k}+\sum_{j\in C^k} QS_{m,k}=QC_{j,k} \tag{22}$$

$$\sum_{n\in w^k} QH_{i,n,k}=CW_{n,k} \tag{23}$$

where $QH_{i,k}$ is the heat content of hot stream *i* at temperature interval *k*, $Q_{i,j,k}$ is the heat transferred from hot stream *i* to cold stream *j*, $Q_{i,n,k}$ is the heat transferred from hot stream to cold utility *n*, $QS_{m,k}$ is the heat content of hot utility *m* at temperature *k*, $QS_{m,j,k}$ is the heat transferred from hot utility stream *m* to cold stream *j* at interval *k*, $RH_{i,k}$ is the heat residual of hot stream *i* from temperature interval *k*, $RS_{i,k}$ is the heat residual of hot utility *m* from temperature interval *k*.

The optimal solution with minimum utility consumption and the links of hot and cold streams at each interval are achieved through the above model. Hot utility consumption was found to be 411.901 kW while cold utility consumption was 62.77 kW. Twenty-four heat exchangers were found to be required to construct the optimal network. It is important to note that this is larger than the original design. Since it is desirable not only to the minimum utility consumption but also to the number of heat exchangers, a new study was implemented with this objective as discussed in the following section.

The expanded transshipment model with logical constraints

Binary variables are included in this model to represent the possibility of heat transfer between hot and cold streams. These binary variables stand for the number of heat exchangers. Prior to building the final model, the whole heat exchange network is first split into two sub-networks at the 'pinch' point, and then in each sub-network the energy balances are set between each stream. This is based on the same approach as that of the previous model and results in a similar model. The objective function is changed to minimize the number of heat exchangers (Eq. (24)) and logical constraints are added in this model (Eqs (25)–(27)). Hot and cold utility consumptions at each temperature interval are predetermined as constants with the same value as optimal results achieved in Section 4.7.

Objective function:

$$\min.\sum_{i}\sum_{j}Y_{i,j}+\sum_{i}\sum_{n}Y_{i,n}+\sum_{m}\sum_{j}YS_{m,j} \tag{24}$$

where

$$Y_{i,j}=\left\{\begin{array}{l}1,\ \text{heat transferred from hot stream } i \text{ to}\\ \text{cold stream } j\\ 0,\ \text{no heat transferred from hot stream } i \text{ to}\\ \text{cold stream } j\end{array}\right\}$$

$$Y_{i,n}=\left\{\begin{array}{l}1,\ \text{heat transferred from hot stream } i \text{ to}\\ \text{cold utility } n\\ 0,\ \text{no heat transferred from hot stream } i \text{ to}\\ \text{cold stream } n\end{array}\right\}$$

$$YS_{m,j}=\left\{\begin{array}{l}1,\ \text{heat transferred from hot utility } n \text{ to}\\ \text{cold stream } j\\ 0,\ \text{no heat transferred from hot utility } n \text{ to}\\ \text{cold stream } j\end{array}\right\}$$

Logical constraints:

$$\sum_{k}Q_{i,j,k}-U_{i,j}Y_{i,j}\leq 0 \tag{25}$$

$$\sum_{k}Q_{i,n,k}-U_{i,n}Y_{i,n}\leq 0 \tag{26}$$

$$\sum_{k}QS_{m,j}-US_{m,j}Y_{m,j}\leq 0 \tag{27}$$

where $U_{i,j}$ is the upper limit of heat transferred between cold stream j and hot stream j at interval k. Similarly, $U_{i,n}$, $US_{m,j}$ are the upper limits of heat transferred from hot streams i to cold utility n and hot utility m to cold streams j, respectively.

The purpose of logical constraints is to set the logic relations between binary variables and energy balances. So, when Y_{ij} is set to zero, the heat transfer between hot stream i and cold stream j will be automatically reset to the zero by the logical constraints.

As demonstrated in Fig. 3, the solution of the above model resulted in 17 heat exchangers. Hot and cold utilities are 413.214 and 62.770 kW, respectively. Compared to the original design (shown in Fig. 2), the hot utility consumption is reduced by 8.6% while the cold utility is decreased by 38.18%.

Conclusions

In this paper, a brief survey of hydrogen production methods is conducted, and among these methods, thermochemical hydrogen production is considered as the most potential efficient method. As a promising cycle, S–I cycle is studied. To improve the thermal efficiency and capital cost of this process, heat integration is implemented. An LP optimization model is first built to minimize utility consumption, and then an expanded transshipment model is defined to find the links between cold streams and hot streams. Finally a mixed integer model is built to explore the minimum number of heat exchangers. As illustrated in Fig. 3, based on the achieved results from the models above, the optimal network is established.

References

1 Energy Supply and Demand, Statistics Canada, Table 128-0009, Catalogue No: 57-003-x, 2007.

2 K. Tsunokawa and C. Hoban, Roads and Environment, A Handbook, The World Bank, Washington, D. G., 1997, p. 90.

3 Inventory of U. S. Greenhouse Gas Emission and Sinks: 1990-2006 (EPA 430-R-08-005), U. S. Environmental Protection Agency, Washington, D.C., 2008, p. ES-15.

4 Fuel Cell Vehicle World Survey 2003, Breakthrough Technologies Institute, Washington, D.C., 2004, pp. 55, 57, 82.

5 A. Tugnoli, G. Landucci and V. Cozzani, Int. J. Hydrogen Energy, 33 (2008) 4352.

6 Y. Z. Chen, Y. Z. Wang, H. Y. Xu and G. X. Xiong, Appl. Catal. B: Env., 80 (2008) 283.

7 J. Ivy, Summary of Electrolytic Hydrogen Production, Milestone Completion Report National Renewable Energy Laboratory, U.S. Department of Commence, Springfield VA, 2004, p. 8.

8 EN19 Efficiency of conventional thermal electricity production, European Environment Agency, 2007, p. 3.

9 J. S. Herring, J. E. O'Brien, C. M. Stoots, G. L. Hawkes, J. J. Hartvigsen and M. Shahnam, Int. J. Hydrogen Energy, 32 (2007) 441.

10 C. W. Forsberg, Int. J. Hydrogen Energy, 28 (2003) 1075.

11 S. Kasahara, S. Kubo, R. Hino, K. Onuki, M. Nomura and S. Nakao, Int. J. Hydrogen Energy, 32 (2007) 489.

12 B. Yidiz and M. S. Kazimi, Int. J. Hydrogen Energy, 31 (2006) 83.

13 P. M. Mathias, General Atomics and Sandia National Laboratories Modeling the Sulfur-Iodine, Aspen Plus Building Blocks and Simulation Models, AspenTech, Rev. 2, 2002, p. 4.

14 K. Schultz, Thermochemical Production of Hydrogen from Solar and Nuclear Energy, General Atomics, San Diego, 2003, pp. 7, 30.

15 B. Belaissaoui, R. Thery, X. M. Meyer, M. Meyer, V. Gerbaud and X. Joulia, Chem. Eng. Process., 47 (2008) 397.

16 L. C. Brown, G. E. Besenbruch, R. D. Lentsh, K. R. Schultz, J. F. Funk, P. S. Pickard, A. C. Marshall, S. K. Showalter, High Efficiency Generation of Hydrogen Fuels Using Nuclear Power, General Atomics, 2003, pp. iii, 3–7, 3–13, 3–, 3–16.

17 R. Turton, R. C. Bailie, W. B. Whiting and J. A. Shaeiwitz, Analysis Synthesis and Design of Chemical Processes, Second Edition, Prentice Hall PTR, New Jersey, 2007, pp. 464–477.

18 L. T. Biegler, I. E. Grossmann and A. W. Westerberg, Systematic Methods of Chemical Process Design, Prentice Hall PTR, New Jersey, 1997, pp. 527–566.

DOI: 10.1007/s10973-008-9834-0